

Supporting Information

A porous and redox active ferrocenedicarboxylic acid based aluminium MOF with MIL-53-architecture.

Jannik Benecke, Sebastian Mangelsen, Tobias Engesser, Thomas Weyrich, Jannik Junge, Norbert Stock, and Helge Reinsch*

Institute of Inorganic Chemistry, Christian-Albrechts-Universität, Max-Eyth Straße 2, D-24118 Kiel, Germany.

Index

1 Experimental	3
1.1 Chemicals.....	3
1.2 Synthesis.....	3
1.3 Characterisation	5
1.3.1 Powder X-Ray Diffraction	5
1.3.2 IR Spectroscopy	5
1.3.3 UV/VIS Spectroscopy.....	5
1.3.4 ¹ H-NMR Spectroscopy	5
1.3.5 EDX and ESEM	5
1.3.6 Optical Microscopy.....	5
1.3.7 Elemental Analysis.....	5
1.3.8 Thermogravimetry.....	5
1.3.9 N ₂ - and H ₂ O-Sorption Measurements	5
1.3.10 ESR Spectroscopy	5
1.3.11 Mößbauer Spectroscopy	5
1.3.12 Cyclic Voltammetry	6
1.4 Rietveld Refinement.....	6
2 XRD-and VTXRD Measurements.....	7
3 Crystal Structure of Al-MIL-53-FcDC.....	8
4 SEM Micrographs and EDX Measurements.....	10
5 IR-Spectroscopy	12
6 Thermogravimetry.....	14
7 PRXD Measurement after Sorption- and TG- experiments.....	16
8 CHN-Analysis	17
9 ¹ HNMR Spectroscopy	18

10 Chemical Stability of Al-MIL-53-FcDC.....	19
11 Additional Data Cyclic Voltammetry	20
12 References.....	21

1 Experimental

1.1 Chemicals

All chemicals are commercially available and were used as received. It should be mentioned that the synthesis of Al-MIL-53-FcDC works particularly well with the linker molecule purchased from Alfa Aesar. In Table 1 the used chemicals are listed.

Tab. S1 List of used chemicals with supplier and purity level.

Chemical	Producer	Purity Level
Acetone	Walter	pure
Acetonitrile	Fischer	99%
Aluminum(III)sulfate 18-hydrate	Kraft	pure
DMF	Grüssing	pure
Acetic Acid	VWR	99 %
1,1-Ferrocenedicarboxylic Acid	Alfa Aesar	99 %
NaOD in D ₂ O (40 %)	Deutero	-
Nafion (in aliphatic alcohols and water(5 wt.%))	Sigma Aldrich	-

1.2 Synthesis

The compound Al-MIL-53-FcDC-as was synthesised employing a molar ratio of 1:1 for H₂FcDC (11.3 mg, 0.0412 mmol) and aluminum sulfate octadeca-hydrate (27.3 mg, 0.0412 mmol). The reactants were placed in a Duran®-glass reactor (Volume 4 mL). A mixture of water (300 µL) and DMF (300 µL) was added. In the next step 10 µL (0.175 mmol) of acetic acid and a magnetic stirring bar were placed in the Duran®-glass reactor. A scale up of the synthesis of Al-MIL-53-FcDC could also be achieved. For this approach, a larger Duran®-glass reactor (8 mL) was used. The synthesis mixture was composed of the starting materials H₂FcDC (56.5 mg, 0.2060 mmol) und Al₂(SO₄)₃ · 18 H₂O (137.0 mg, 0.2060 mmol), the modulator acetic acid (50 µL, 0.875 mmol) and the solvent mixture, consisting of water (1.5 mL) and DMF (1.5 mL). The reactors were sealed and placed in an aluminium block (Fig S1) and heated up to 95°C for 90 min under stirring. After cooling down, the reaction products were filtered off and the obtained light brown powders were washed with a mixture of DMF and water (1:1 ratio). In addition to a fine powder, a second reaction product of Al-MIL-53-FcDC with a different morphology was obtained, which formed agglomerated at the inner site of the glass reactor (Fig S1 right). This product was removed manually and also washed with the DMF/water mixture. Characterisation by PXRD, elemental analysis, IR spectroscopy and thermogravimetry showed only subtle differences between the different morphologies, nevertheless the further experiments discussed in the manuscript were carried out exclusively using the fine powder.

For the CV experiment the MOF was deposited in a matrix of the copolymer Nafion on the gold electrode. Therefore, the MOF (8 mg) was dispersed in a solution consisting of ethanol, water and Nafion (1 mL, 6 mL and 30 µl, respectively) in an ultrasonic bath. Afterwards a liquid film of the MOF dispersion was deposited on the electrode and dried in air over night. This procedure was repeated twice.

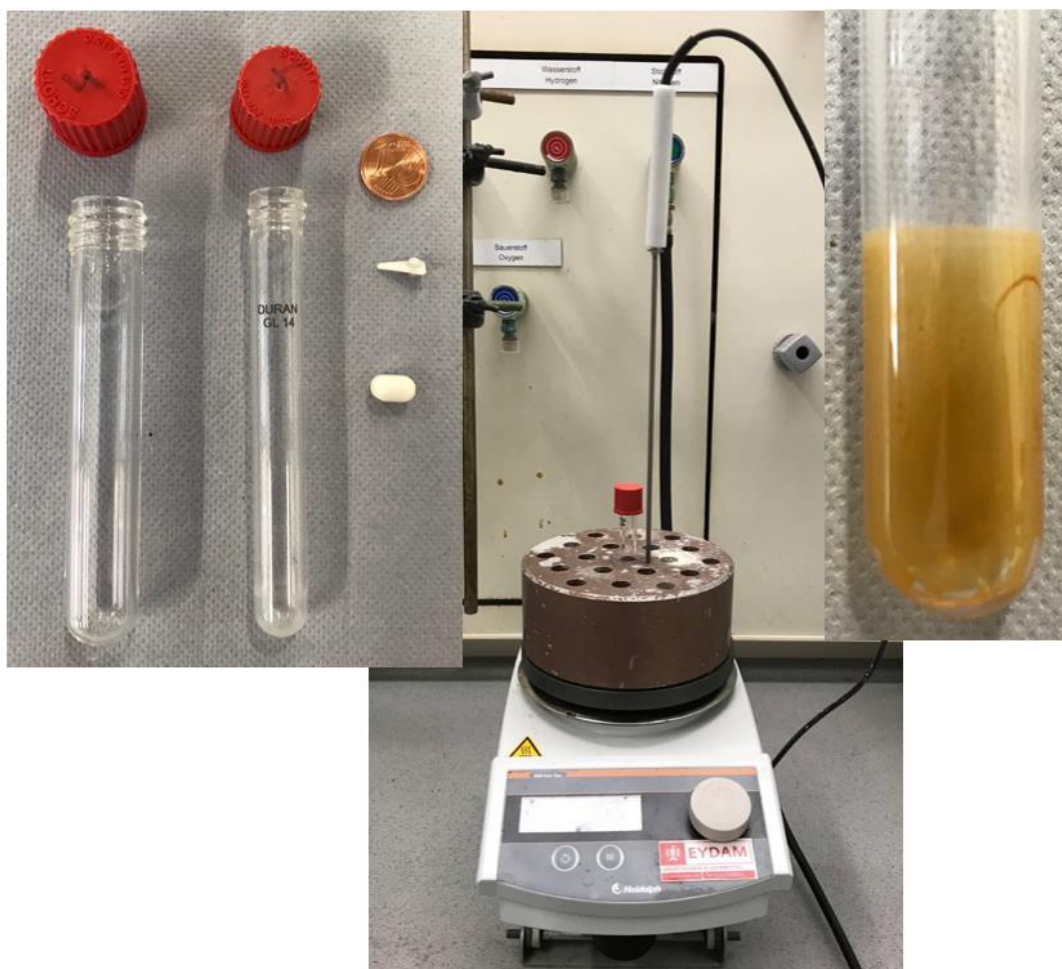


Fig. S1 Left: Photography of the used Duran® glass reactors (left: 8 mL und right 4 mL) with the respective magnetic stirring bar and the red sealing caps. Centre: Photography of the set up with the used heating plate and aluminium block. Right: Photography of the reactor with agglomerated reaction product.

1.3 Characterisation

1.3.1 Powder X-Ray Diffraction

Different powder diffractometers were used in this work. For high resolution and PXRD pattern measurements after sorption and thermogravimetric experiments, a STOE Stadi-MP powder diffractometer (Cu K α 1 radiation) was used. Furthermore, the variable temperature (VT) PXRD measurements were performed in transmission geometry with a STOE Stadi-P combi powder diffractometer (Cu K α 1 radiation) equipped with a capillary furnace. Therefore the samples were placed in a 0.5 mm quartz capillary. The PXRD experiment of the MOF deposited on gold electrode was performed with a Panalytical X'Pert Pro MPD equipped with Göbel mirror and a PIXCel 1D using Cu K α radiation in reflection geometry.

1.3.2 IR Spectroscopy

The IR Spectra of the samples were recorded with a Bruker ALPHA-FT-IR A220/D-01 spectrometer using an ATR-unit.

1.3.3 UV/VIS Spectroscopy

The UV/VIS spectra were recorded with an Agilent UV/VIS-NIR-spectrometer in reflection geometry. Prior to the measurement the powders were mixed with BaSO₄.

1.3.4 ¹H-NMR Spectroscopy

The ¹H-NMR spectra of the samples were recorded on a Bruker DRX 500 spectrometer. For the measurements the samples were dissolved in a 10% NaOD / D₂O-solution.

1.3.5 EDX and ESEM

The EDX measurements were performed with a Gemini Ultra55Plus analyser equipped with an Oxford SD-Detector. Micrographs were recorded using a Philips ESEM XL 30.

1.3.6 Optical Microscopy

The pictures of MOF coated gold electrodes were recorded with a Olympus BX50 microscope.

1.3.7 Elemental Analysis

CHNS contents were determined with a HEKAtech Euro EA Elemental Analyser.

1.3.8 Thermogravimetry

The thermogravimetric measurements were performed using a NETZSCH STA 409 CD analyser. The flow of air was adjusted to 75 mL/min. The heating rate for the TG measurement amounts to 4°C/min.

1.3.9 N₂- and H₂O-Sorption Measurements

The sorption experiments were performed with a BEL Japan Inc. BELSORP-max (Nitrogen (77 K) and water vapour (298 K)).

1.3.10 ESR Spectroscopy

All ESR spectra were measured with a Bruker EMXplus spectrometer with a PremiumX microwave bridge and a Bruker HQ X-Band cavity. The measured experiments were performed at X-Band microwave radiation of 9.86 GHz. For the measurement, the powder was measured in solid state at room temperature.

1.3.11 Mößbauer Spectroscopy

The Mößbauer spectrum was measured on a custom made Mößbauer spectrometer. The spectrum was recorded in linear transmission geometry. As the power unit, the "Mößbauer Drive System MR206A" and the "Mößbauer Velocity Transducer MVT-1000" from the company "Wissenschaftliche

Elektronik GmbH" in Starnberg were used. As the source of radiation, ^{57}Co in a Rhodium matrix with a starting activity of 25mCi was used. All shifts are denoted relative to α -iron. The resulting spectra were fitted with the software FitSuite 1.0.4.

1.3.12 Cyclic Voltammetry

The cyclic voltammograms were measured on an EG&G Princeton Applied Research/Model 273A using an Ag rod as a pseudo reference electrode and Pt as counter electrode. The MOF coated gold electrode consists of a glass substrate with a 50 \AA titanium adlayer and a 200 nm evaporated gold film on the surface. A solution of 0.1 M NaPF₆ in acetonitrile was used as electrolyte. As reference a minute amount of ferrocene was dissolved in the electrolyte and a CV was recorded with a blank gold electrode.

1.4 Rietveld Refinement

While the PXRD pattern of the activated sample matches also with higher symmetry than triclinic, a refinable structural model could be only set up in *P*-1 symmetry. A triclinic cell matching with the pattern was identified by indexing with TOPAS academic ($a = 6.652(2)$, $b = 10.652(2)$, $c = 10.674(3)$ \AA and $\alpha = 79.32(2)$, $\beta = 71.79(2)$, $\gamma = 71.81(2)$ $^\circ$).³ Using the crystal structure of the related triclinic framework of CAU-13 as starting point, the linker molecules were replaced by ferrocene, the indexed parameters were imposed and the thus obtained structural model was optimised by force-field calculations using Materials Studio.¹ This initially obtained model could be refined by Rietveld methods using TOPAS academics.³ The organic moieties were refined as rigid bodies, while all other atoms were freely refined, using only distance restraints. Some residual electron density inside the pores was attributed to oxygen atoms with refinable occupancy, representing any kind of guest molecule. In addition, a slight preferred orientation along [001] was also taken into account. The final Rietveld plot is show in the manuscript while some relevant parameters are summarised below in Section 3.

2 XRD-and VTXRD Measurements

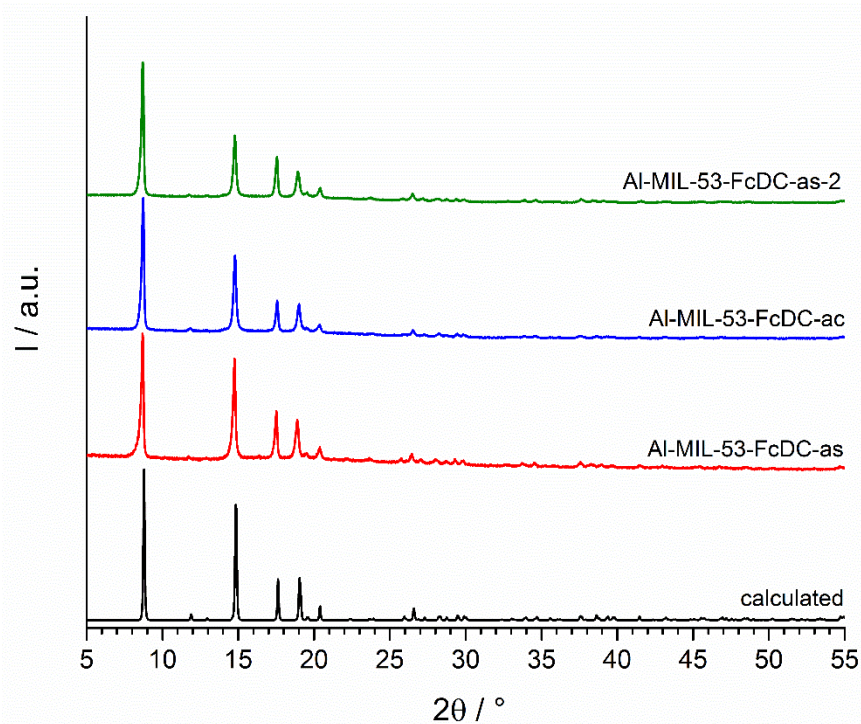


Fig. S2 Calculated PXRD pattern for the title compound (black) and experimental PXRD patterns for as synthesised Al-MIL-53-FcDC-as (red), activated Al-MIL-53-FcDC-ac (blue) and Al-MIL-53-FcDC-as-2 (green), representing the product grown on the reactor walls.

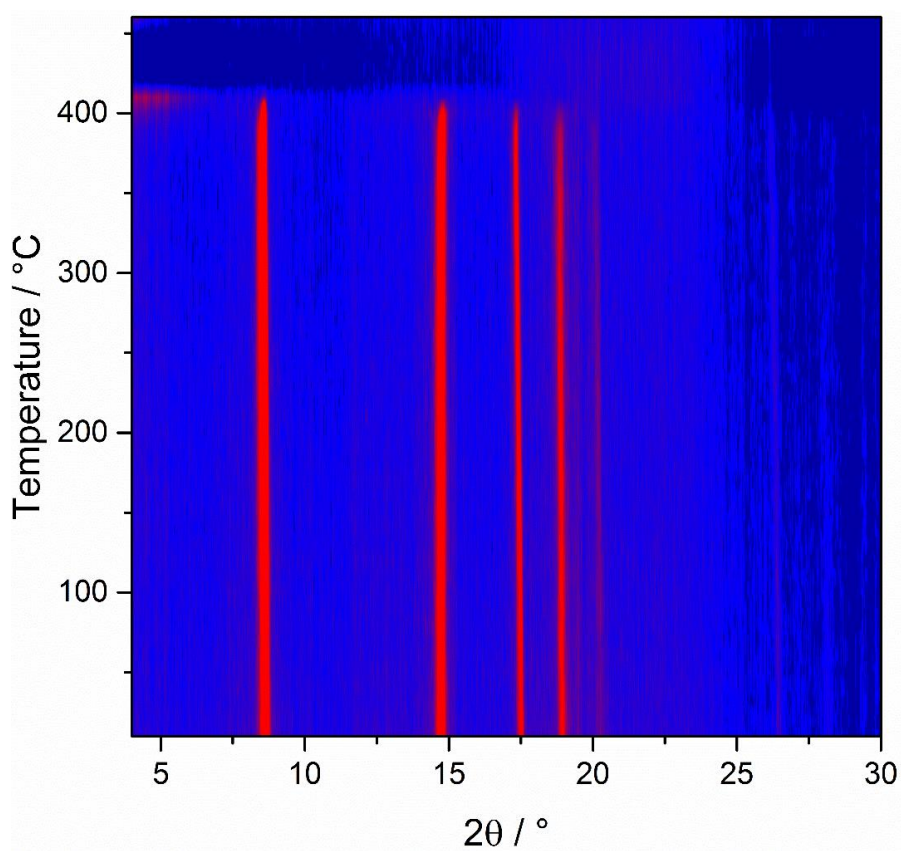


Fig. S3 Results of the variable temperature powder x-ray diffraction investigation of Al-MIL-53-FcDC. The sample was heated up in steps of 10°C between 30°C and 460°C .

3 Crystal Structure of Al-MIL-53-FcDC

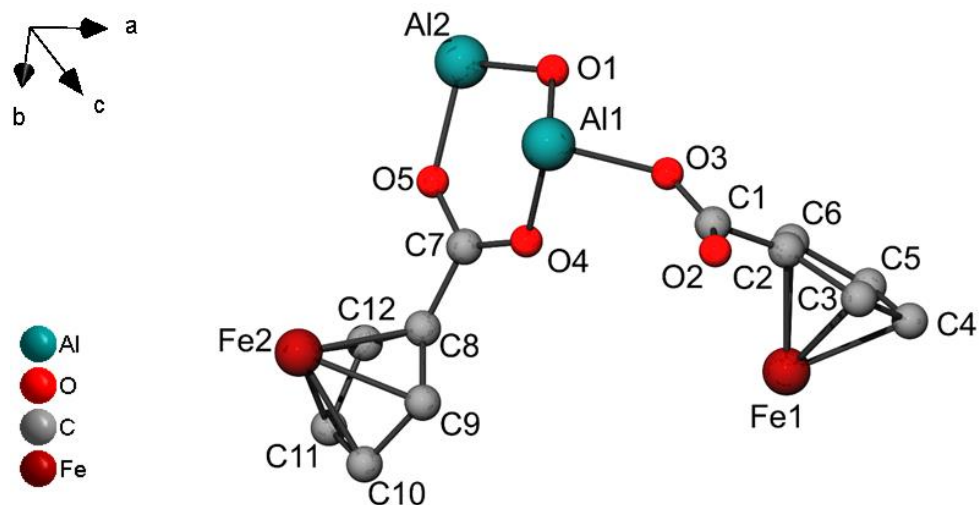


Fig S4 Asymmetric unit of Al-MIL-53-FcDC. For the sake of clarity, the guest atoms are not shown.

Tab. S2 Rietveld refinement data for Al-MIL-53-FcDC.

Formula	$[\text{Al}(\text{OH})(\text{FeC}_{12}\text{H}_8\text{O}_4)] \cdot 1\text{H}_2\text{O}$
Crystal System	Triclinic
Space Group	<i>P</i> -1
<i>a</i> / Å	6.6261(5)
<i>b</i> / Å	10.620(2)
<i>c</i> / Å	10.642(2)
α / °	79.896(13)
β / °	71.512(13)
γ / °	71.851(16)
<i>V</i> / Å ³	672.5(2)
<i>R</i> _{WP} / %	2.4
<i>R</i> _{Exp} / %	1.4
<i>R</i> _{Bragg} / %	0.6
GoF	1.8

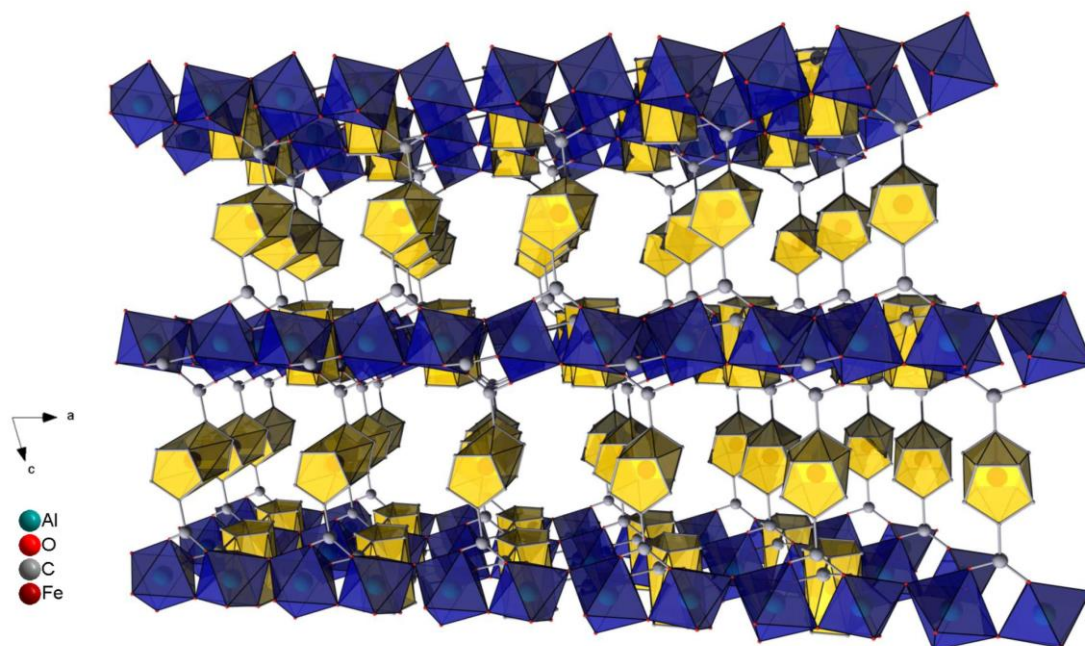


Fig. S5 Representation of the structure of Al-MIL-53-FcDC seen along the *b*-axis.

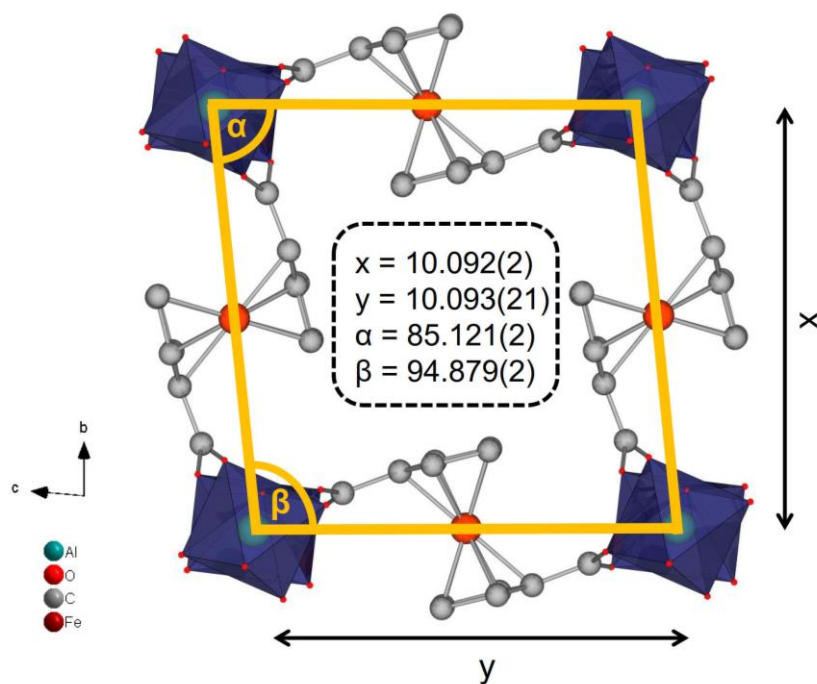


Fig. S6 Representation of distances and angles between the IBUs in the structure of Al-MIL-53-FcDC.

Tab. S3 Comparison of the distances and angles between the IBUs of the phases Al-MIL-53-FcDC, Al-MIL-53*ht* und Al-MIL-53*t*.²

Angle or Distance	Al-MIL-53-FcDC	Al-MIL-53 <i>ht</i>	Al-MIL-53 <i>t</i>
a / Å	10.092(2)	10.515(13)	10.233(211)
b / Å	10.093(21)	10.515(13)	10.233(211)
α / °	85.121(2)	75.077(1)	43.672(146)
β / °	94.879(3)	104.934(1)	136.328(217)

4 SEM Micrographs and EDX Measurements

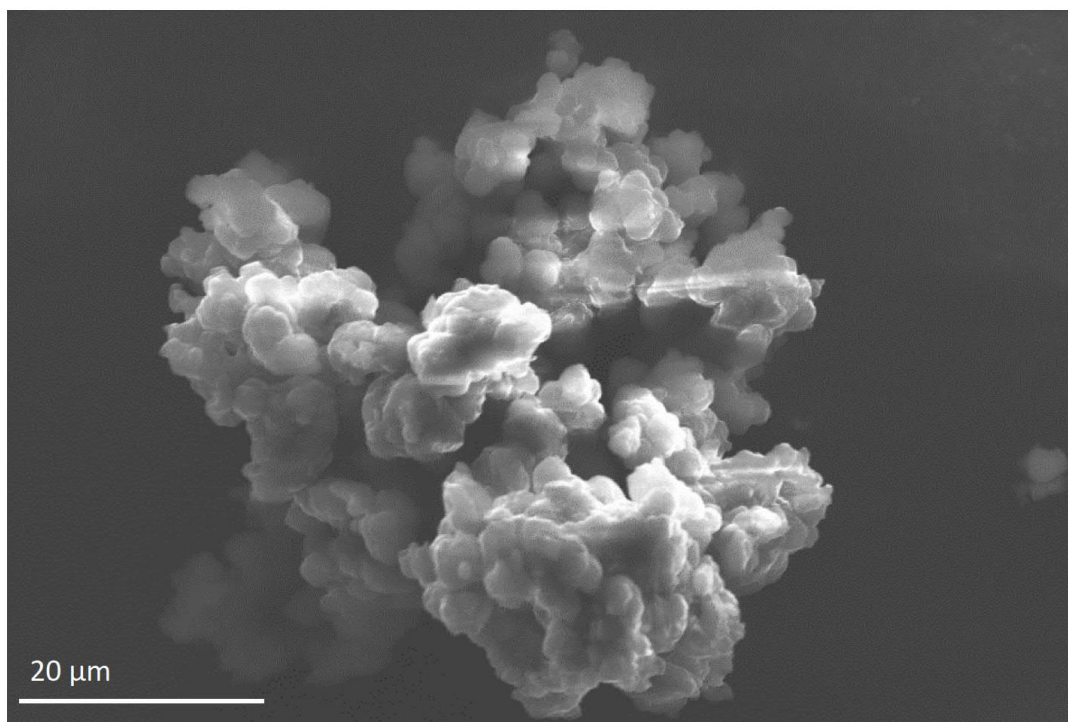


Fig. S7 SEM-micrograph of Al-MIL-53-FcDC-as.

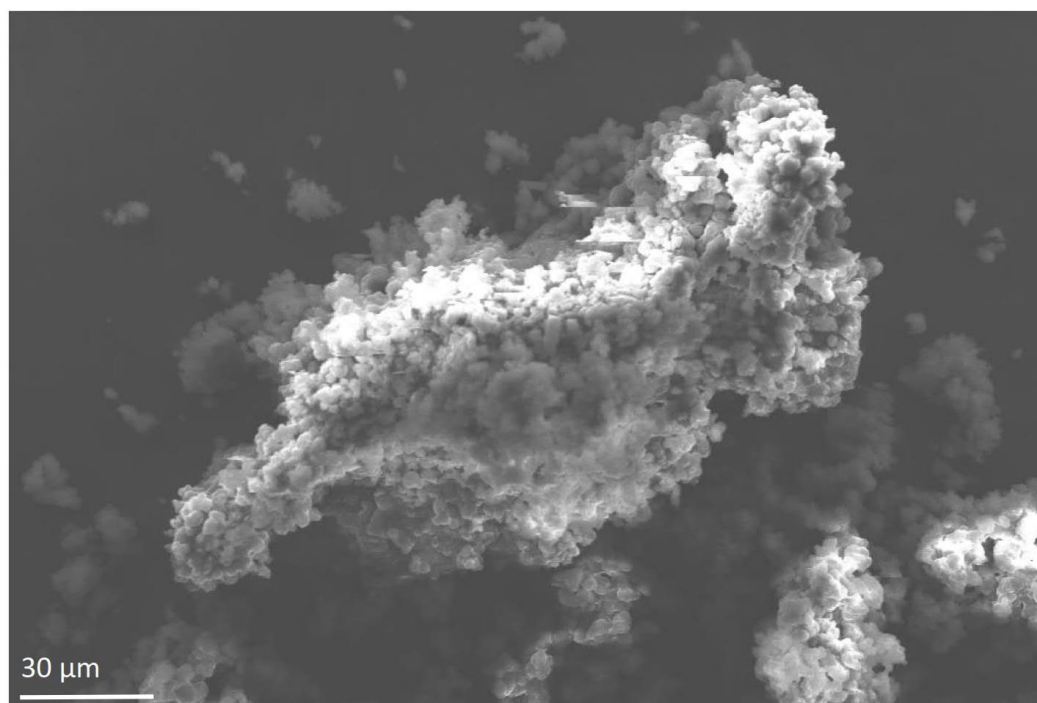


Fig. S8 SEM-micrograph of Al-MIL-53-FcDC-as.

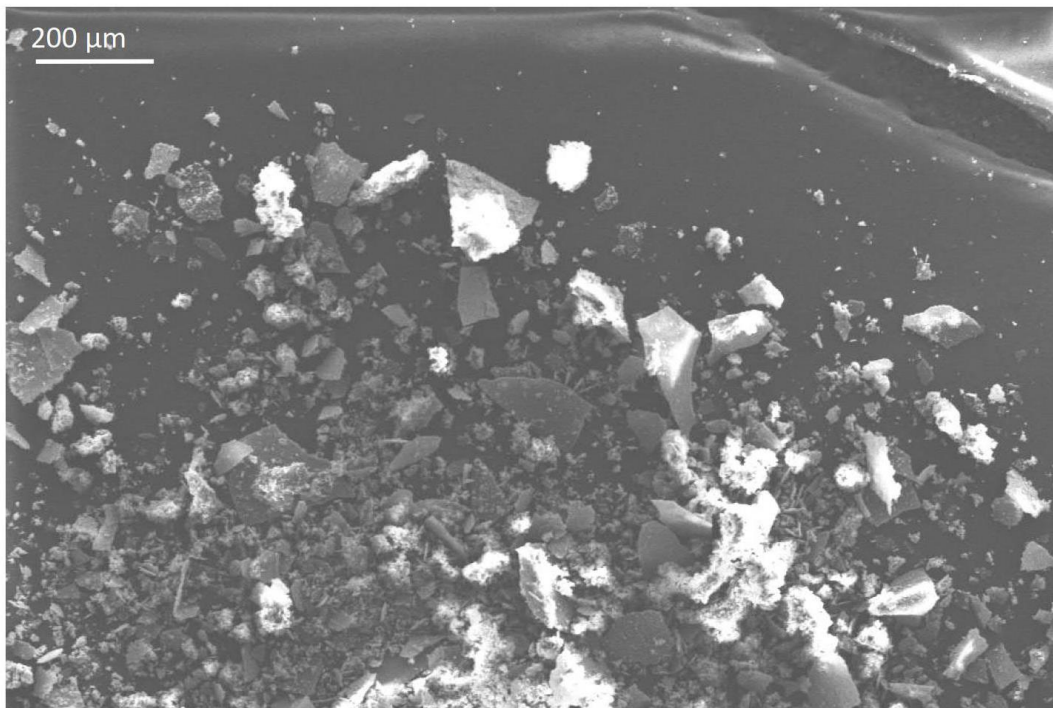


Fig. S9 SEM-micrograph of Al-MIL-53-FcDC-as-2 grown on the reactor wall.

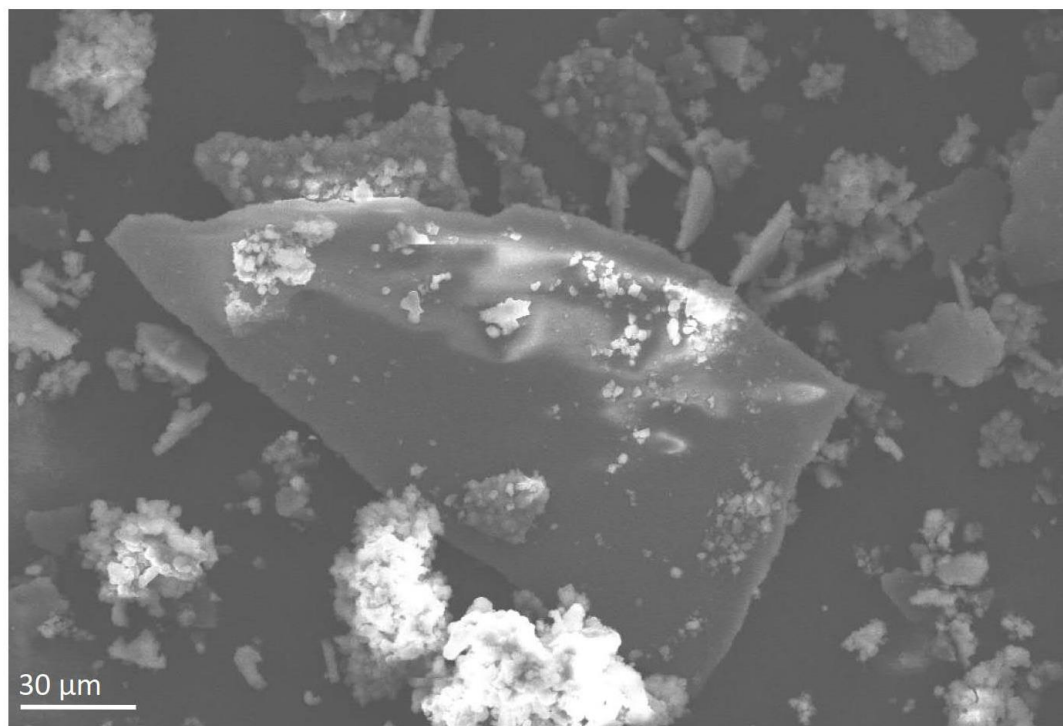


Fig. S10 SEM-micrograph of Al-MIL-53-FcDC-as-2 grown on the reactor wall.

5 IR-Spectroscopy

Tab. S4 Assignment of bands observed in the IR spectrum of Al-MIL-53-FcDC-as and Al-MIL53-FcDC-ac.

Infrared Bands / cm^{-1}	Vibrations
3701	$\nu\text{O-H}$
1674	$\nu\text{C=O DMF}$
1578	$\nu\text{C-O-O}$
1393	$\nu\text{C=C}$
1359	$\nu\text{C-O-O}$
1254	$\nu\text{N-CH}_3$
1205	$\delta\text{C-H}$
1091	$\nu\text{N-CH}_3$
981	$\delta\text{C-H}$

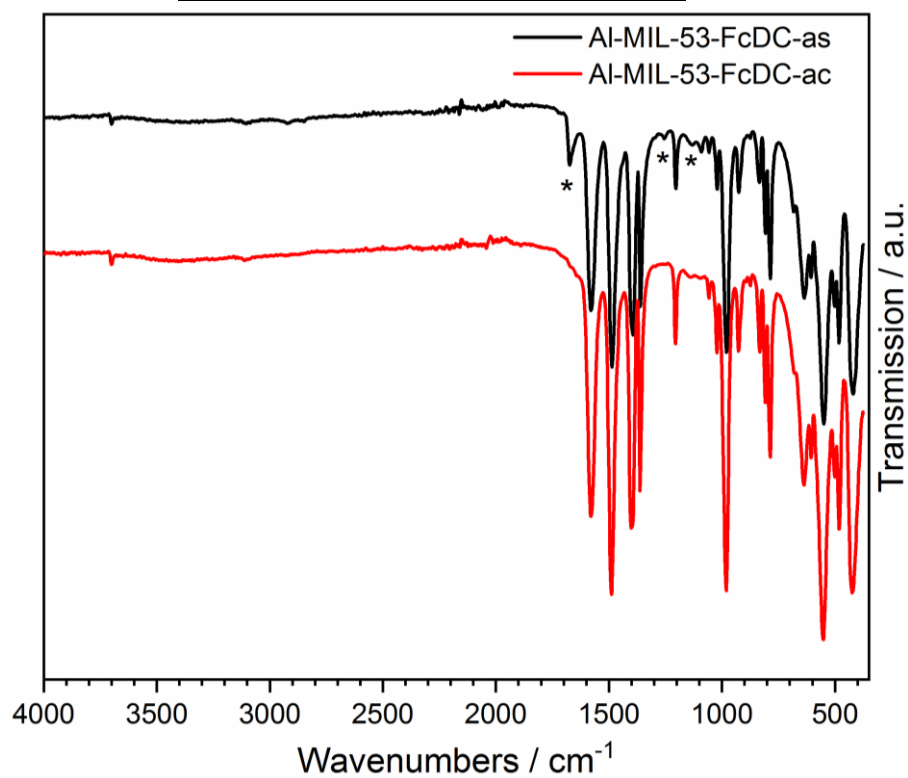


Fig. S11 IR spectra of Al-MIL-53-FcDC-as and Al-MIL-53-FcDC-ac. The asterisks are indicating the absorption bands of DMF.

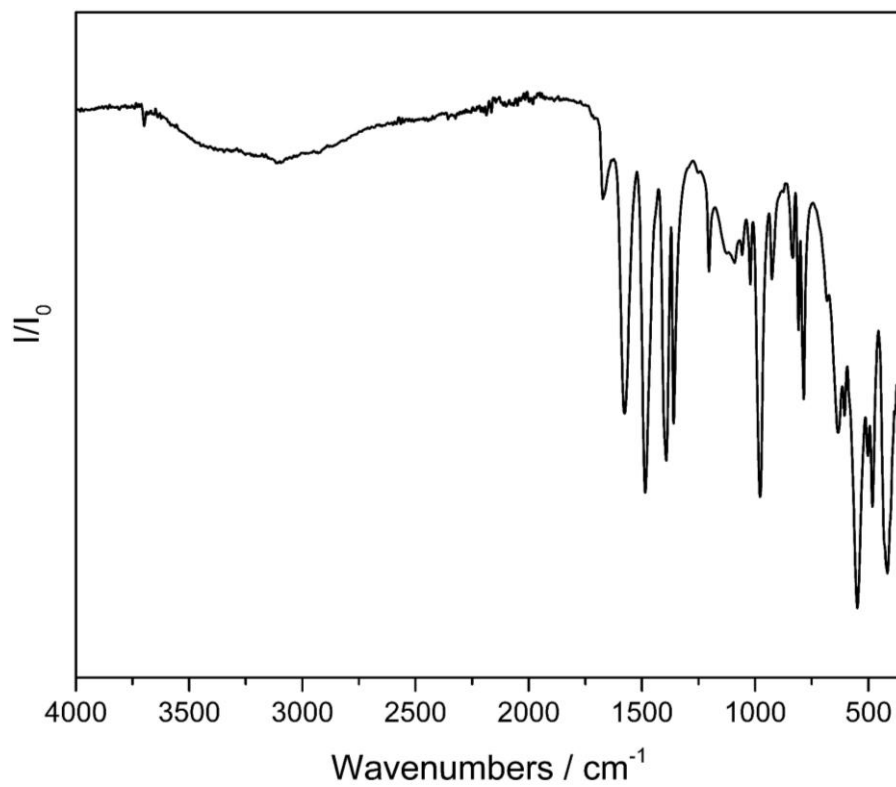


Fig. S12 IR spectrum of Al-MIL53-FcDC-as-2 grown on the reactor wall.

6 Thermogravimetry

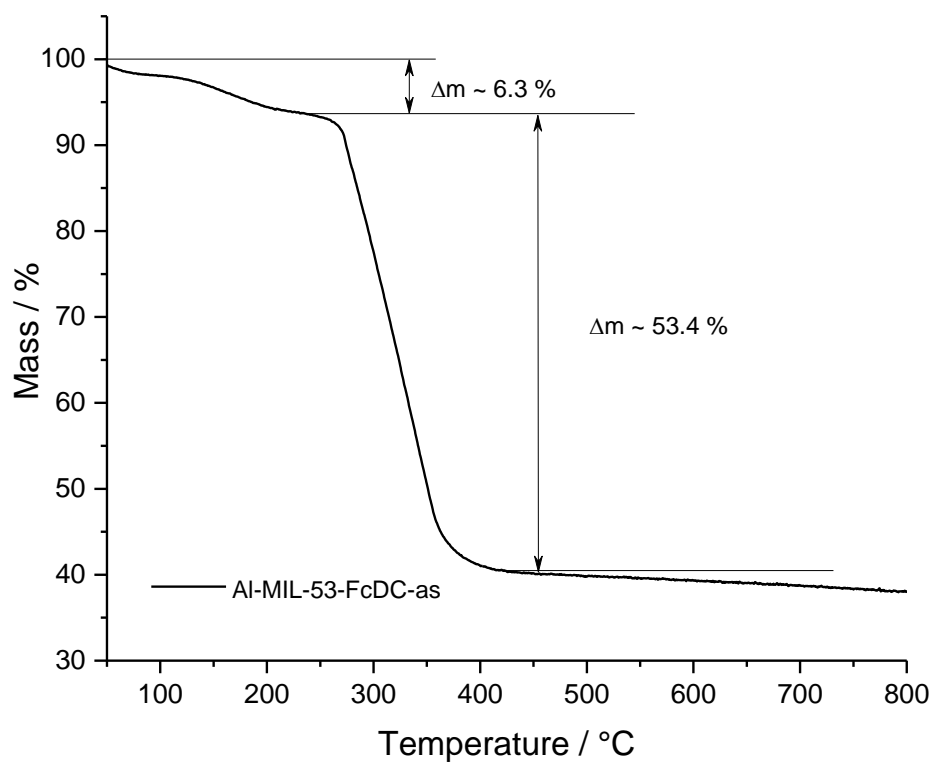


Fig. S13 TG curve of Al-MIL-53-FcDC-as.

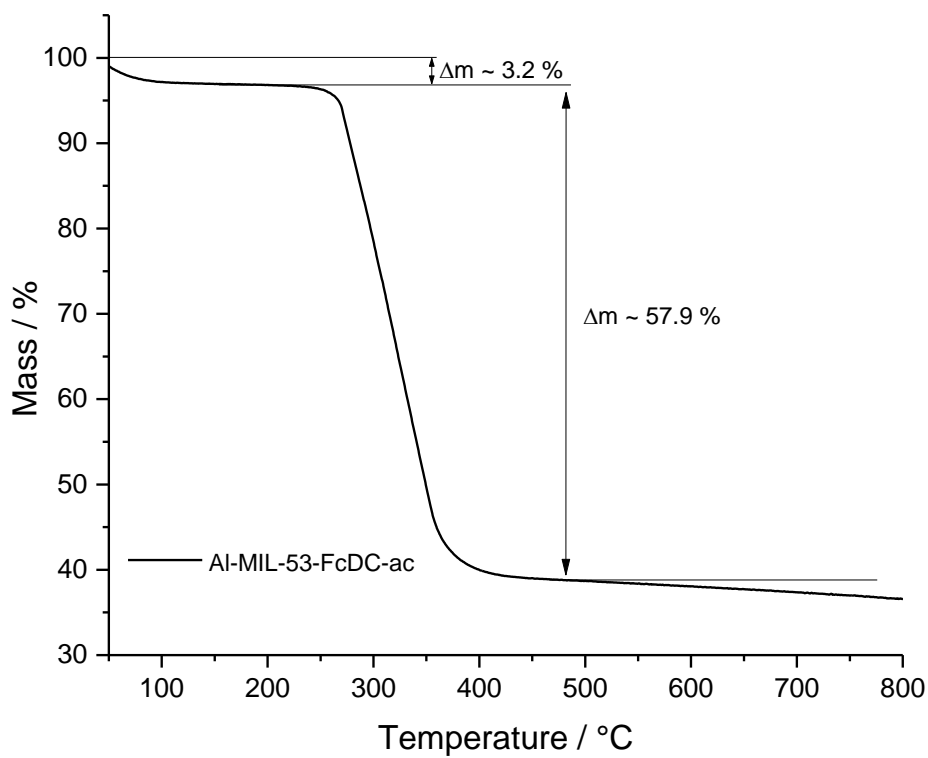


Fig. S14 TG curve of Al-MIL-53-FcDC-ac

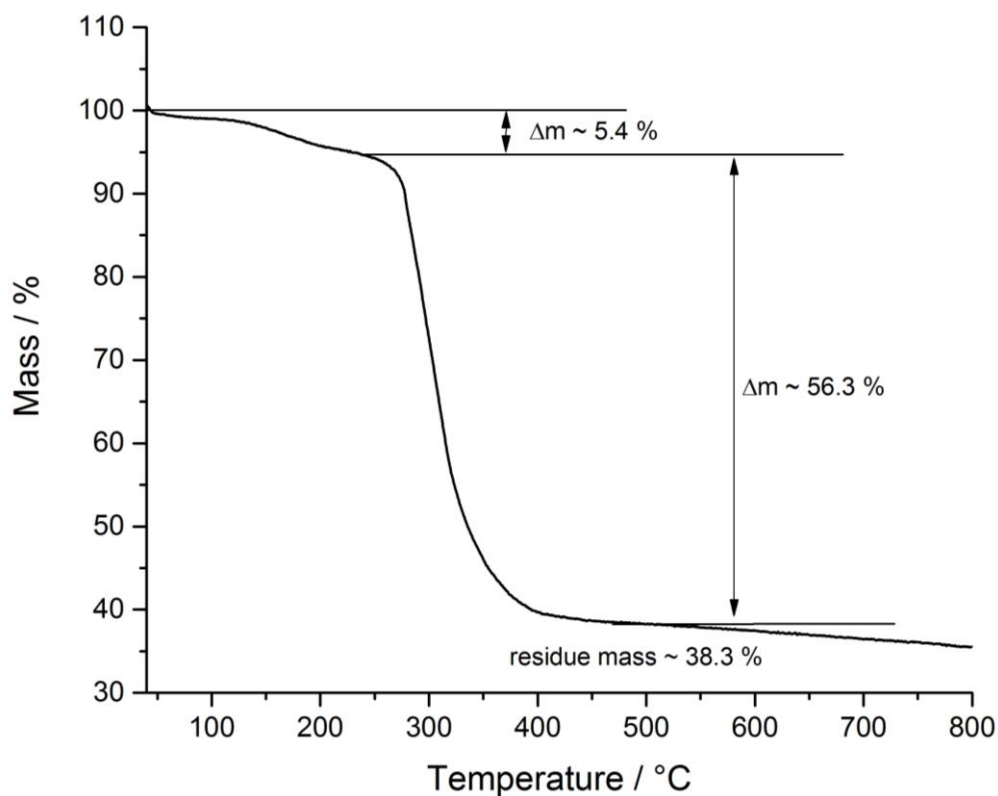


Fig. S15 TG curve of Al-MIL-53-FcDC-as-2.

Tab. S5 Comparison of the measured and calculated mass losses observed in the TG curves of Al-MIL-53-FcDC-as, Al-MIL-53-FcDC-ac and Al-MIL-53-FcDC-as-2.

TG	Measured/ %	Calculated / %	
Al-MIL-53FcDC-as			
Step 1	6.30	6.70	$0.25 \cdot \text{H}_2\text{O} + 0.25 \cdot \text{C}_3\text{H}_7\text{NO}$
Step 2	53.4	54.7	Linker decomposition
Residue	40.3	38.6	$\text{Al}_2\text{O}_3, \text{Fe}_2\text{O}_3$
Al-MIL-53FcDC-ac			
Step 1	3.20	2.80	$0.5 \text{H}_2\text{O}$
Step 2	57.9	57.0	Linker decomposition
Residue	38.9	40.3	$\text{Al}_2\text{O}_3, \text{Fe}_2\text{O}_3$
Al-MIL-53FcDC-ac2			
Step 1	5.4	6.70	$1 \text{H}_2\text{O}$
Step 2	56.3	54.7	Linker decomposition
Residue	38.3	38.6	$\text{Al}_2\text{O}_3, \text{Fe}_2\text{O}_3$

7 PRXD Measurement after Sorption- and TG- experiments

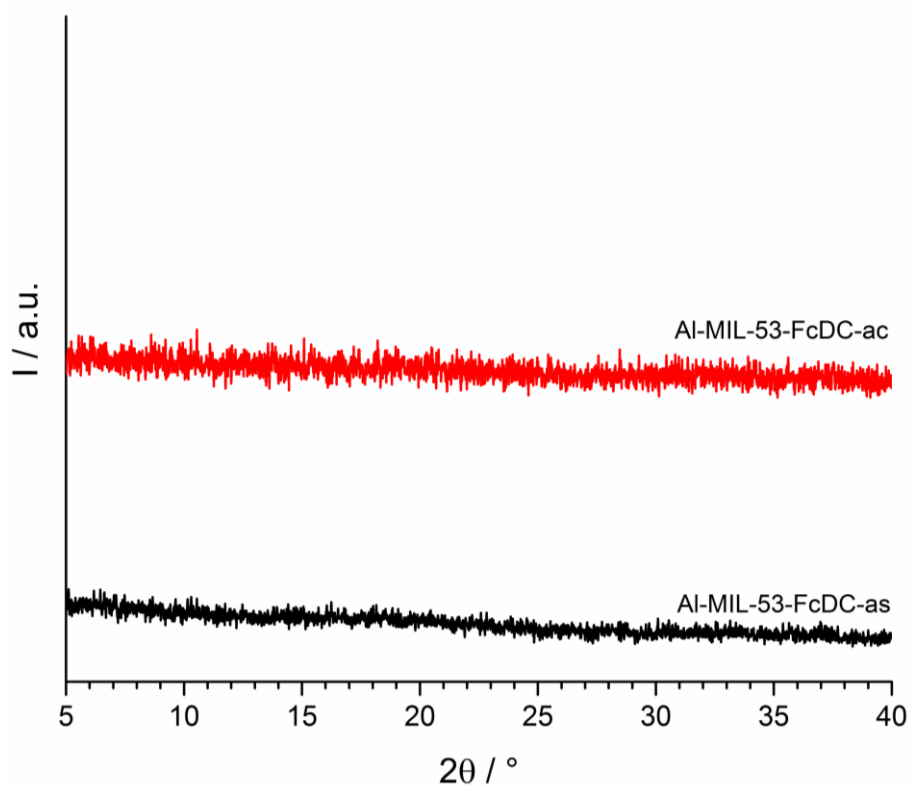


Fig. S16 PXRD patterns of the thermogravimetric residues of Al-MIL-53-FcDC-as (black) and Al-MIL-53-FcDC-ac (red).

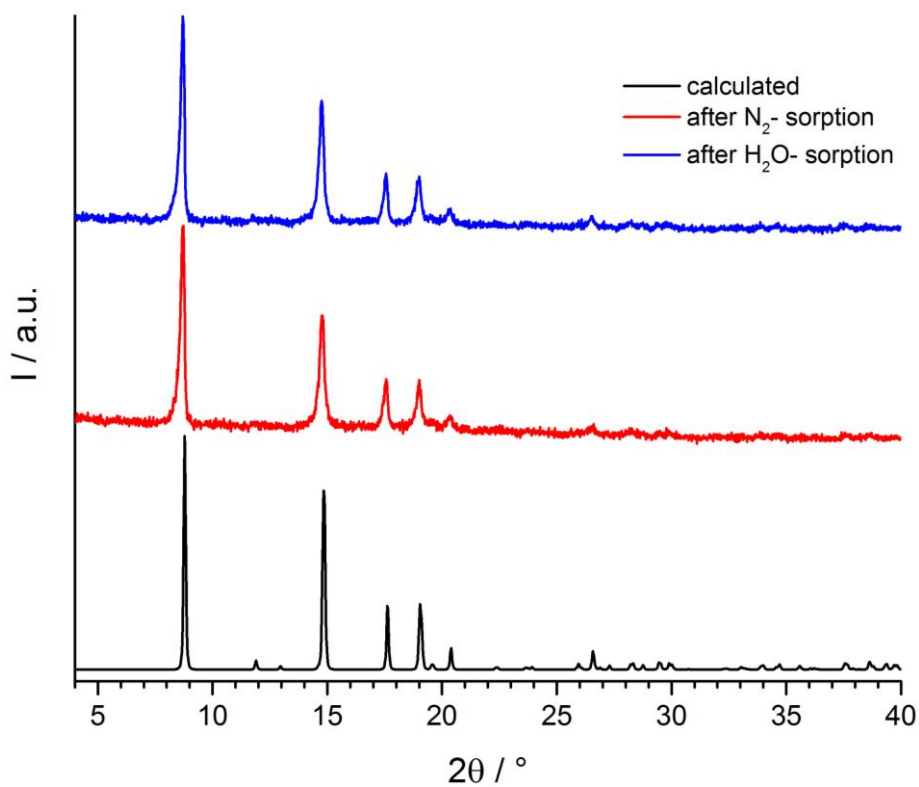


Fig. S17 PXRD patterns of Al-MIL-53Fcdc after N₂ sorption (red) and after H₂O sorption (blue) in comparison to the calculated PXRD pattern of Al-MIL-53-FcDC (black).

8 CHN-Analysis

Tab. S6 Comparison of the measured and calculated CHN values of Al-MIL-53-FcDC-as and Al-MIL-53-FcDC-ac.

Sample	N / wt%	C / wt%	H / wt%
Al-MIL-53-FcDC-as	1.6	43.8	3.7
Calculated $[\text{Al}(\text{OH})(\text{FeC}_{12}\text{H}_8\text{O}_4) \cdot 1 \text{ H}_2\text{O} \cdot 0.5 \text{ C}_3\text{H}_7\text{NO}]$	1.9	43.8	3.9
Al-MIL-53-FcDC-ac	0.0	42.8	3.1
Calculated $[\text{Al}(\text{OH})(\text{FeC}_{12}\text{H}_8\text{O}_4) \cdot 0.5 \text{ H}_2\text{O}]$	0.0	44.3	3.1
Al-MIL-53-FcDC-as-2	1.0	39.9	4.4
Calculated $[\text{Al}(\text{OH})(\text{FeC}_{12}\text{H}_8\text{O}_4) \cdot 3 \text{ H}_2\text{O} \cdot 0.5 \text{ C}_3\text{H}_7\text{NO}]$	1.7	39.9	4.6

9 $^1\text{H-NMR}$ Spectroscopy

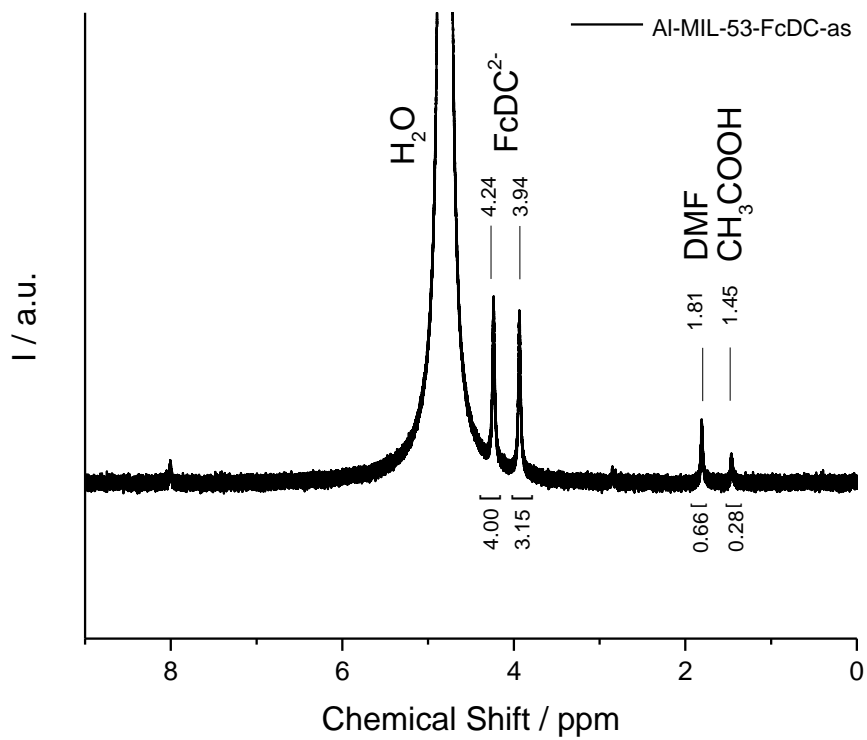


Fig. S18 $^1\text{H-NMR}$ spectrum of Al-MIL-53-FcDC-as.

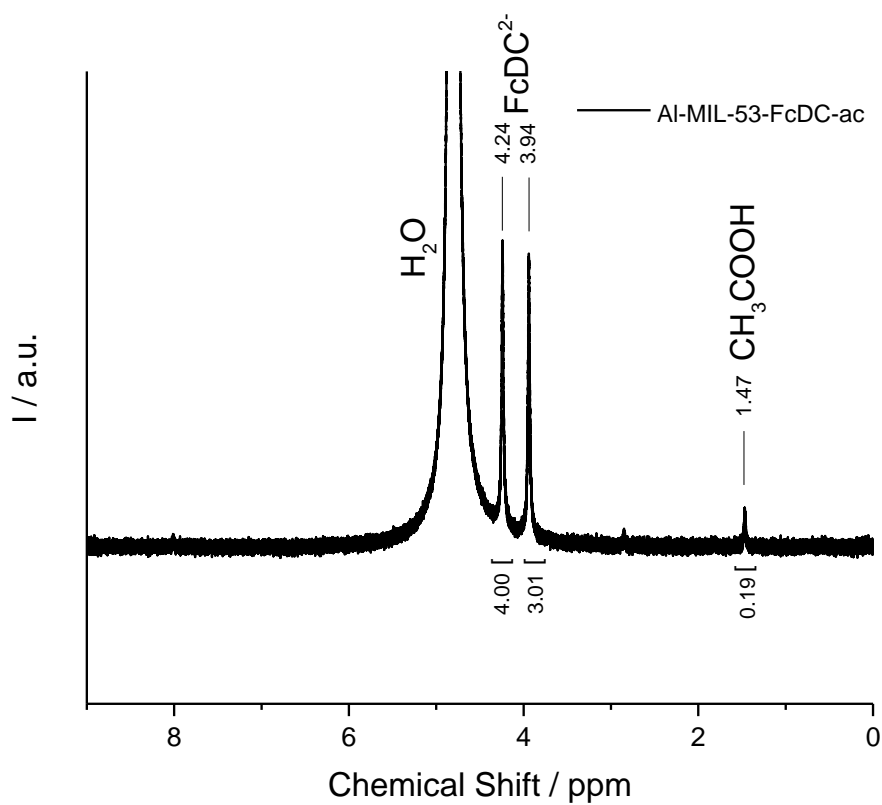


Fig. S19 $^1\text{H-NMR}$ spectrum of Al-MIL-53-FcDC-ac.

10 Chemical Stability of Al-MIL-53-FcDC

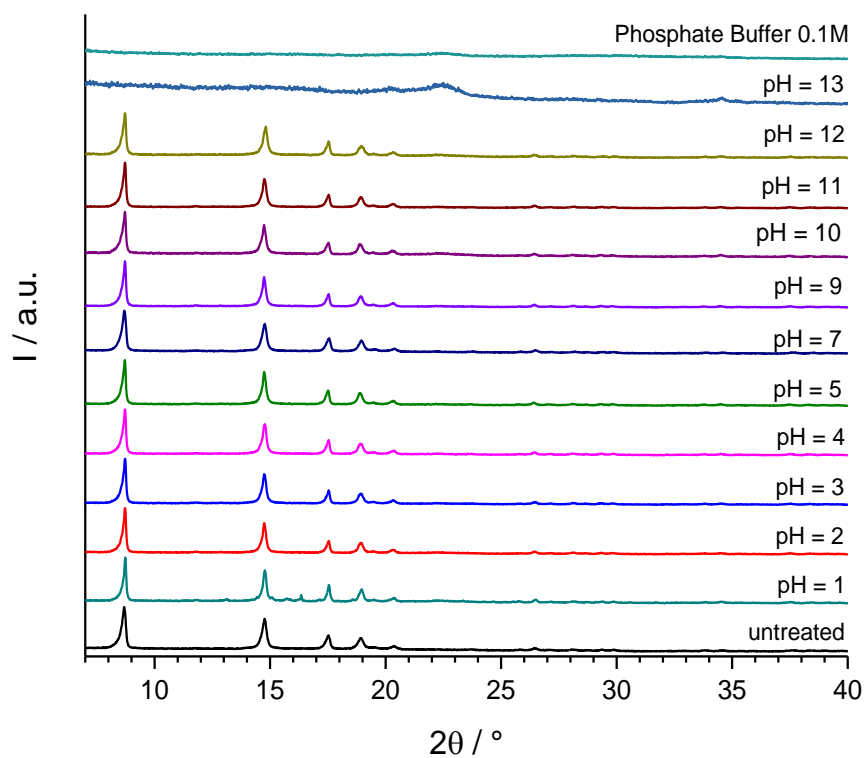


Fig. S20 PXR D patterns of Al-MIL-53FcDC-as treated in different solutions, which were produced by using sodium hydroxide and hydrochloric acid. For the stability tests, 8 mg of Al-MIL-53-FcDC were mixed with 4 mL of the different solutions and stirred for 24 h prior to recovery and measurement.

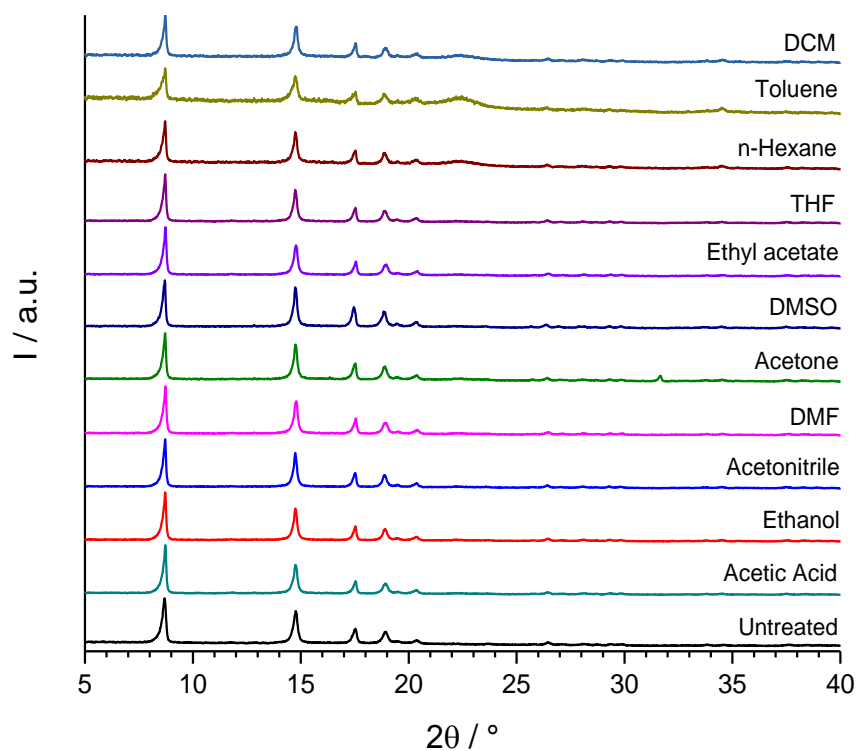


Fig. S21 PXR D patterns of Al-MIL-53FcDC-as after solvent stability tests in organic solvents. 2 mL of the organic substances were added to 8 mg of Al-MIL-53-FcDC, respectively, and were stirred for 24 h prior to recovery and measurement.

11 Additional Data Cyclic Voltammetry

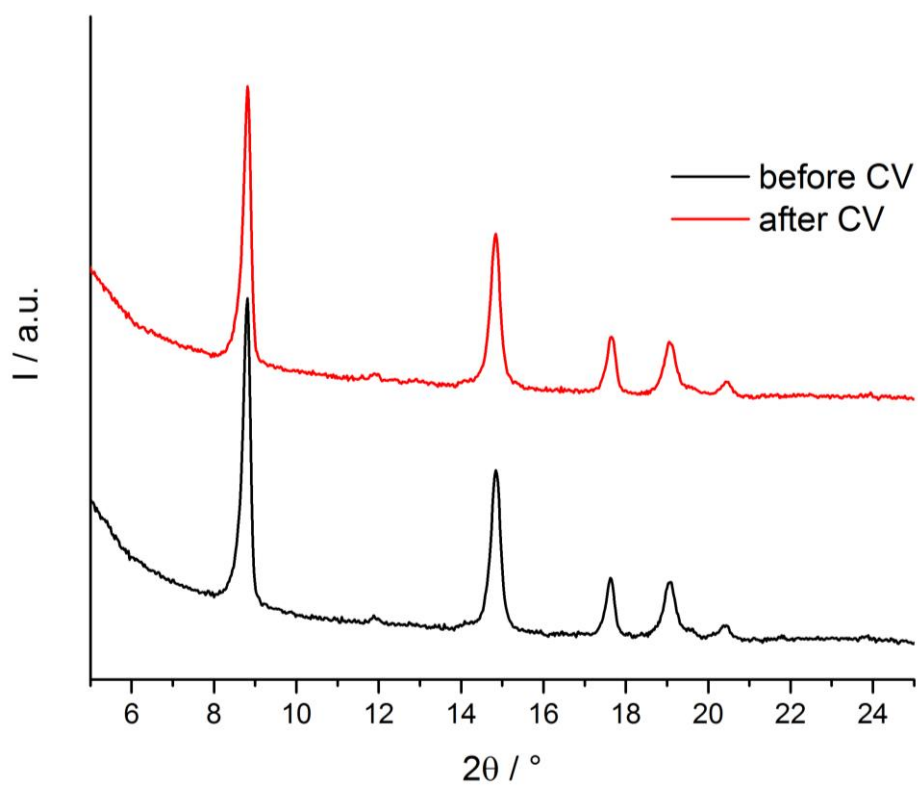


Fig. S22 PXRD patterns of the MOF deposited on gold electrode before (black) and after the CV experiment (red).



Fig. S23 Optical micrograph of Al-MIL-53-FcDC deposited on gold electrode.

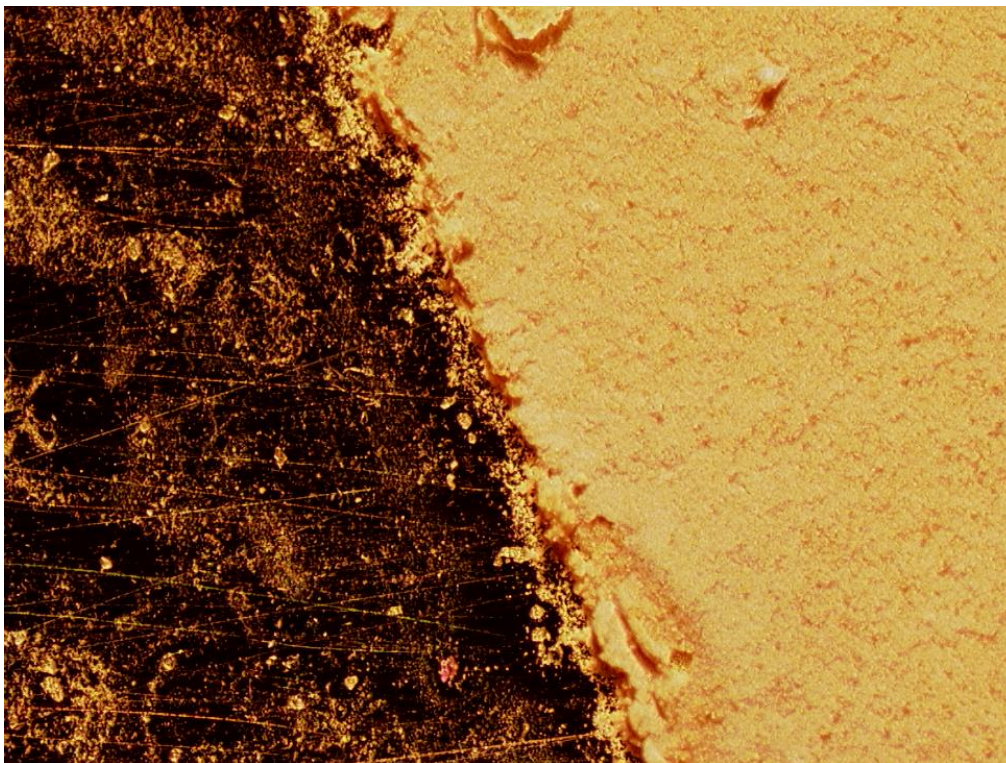


Fig. S24 The optical micrograph shows Al-MIL-53-FcDC (yellow powder) deposited on a gold electrode. The blank electrode surface can be seen in left side of the optical micrograph.

12 References

- 1 Accelrys Inc, Materials Studio Version 5.0, San Diego, 2009.
- 2 T. Loiseau, C. Serre, C. Huguenard, G. Fink, F. Taulelle, M. Henry, T. Bataille and G. Férey, *Chem. Eur. J.*, 2004, **10**, 1373.
- 3 Coelho Software, Topas Academics 4.2, Brisbane, 2007.